THE ASTROPHYSICAL JOURNAL, 411:778–793, 1993 July 10

FAST, LOW-IONIZATION EMISSION REGIONS AND OTHER MICROSTRUCTURES IN PLANETARY NEBULAE

BRUCE BALICK
Astronomy Department, FM-20, University of Washington, Seattle, WA 98195; and Sterrewacht Leiden, Leiden University
M. RUGERS
Astronomy Department, FM-20, University of Washington, Seattle, WA 98195
AND
YERVANT TERZIAN AND JAYARAM N. CHENGALUR
Astronomy Department and National Astronomy and Ionosphere Center, Cornell University, Ithaca, NY 14853
Received 1992 October 12; accepted 1993 January 7

ABSTRACT

Planetary nebulae (PNs) have highly articulated structures, called "microstructures," little of which has been explored with spectrophotometry at high spatial resolution. We report spectrophotometric observations of microstructures characterized by both high signal-to-noise ratio and high spatial resolution (1".5) along the symmetry axes of NGC 3242, NGC 7662, and IC 2149.

Of particular interest in these PNs are pairs of low-ionization and/or high-velocity ansae and jets (fast, low-ionization emission regions [FLIERs]) on nearly opposite sides of their respective central stars, or nuclei (PNNs). We present deep optical spectra of FLIERs in all three PNs and discuss their consequences. The strong low-ionization lines of O°, N^{+}, O^{+}, and S^{+}, substantial space velocities, and temperatures and densities of FLIERs are not well explained either by models of edge-on ionization fronts or by models built on analogies to shock-excited Herbig-Haro objects.

Subject headings: ISM: structure — planetary nebulae: individual (NGC 3242, NGC 7662, IC 2149)

1. INTRODUCTION

Narrow-band images of planetary nebulae (PNs) through filters centered on low-ionization emission lines such as O^{0} and N^{+} (Balick 1987) revealed strange pairs of low-ionization knots and radial "jets" on opposite sides of PNNs along the PN symmetry axis. Balick, Preston, & Icke (1987, hereafter BPI) later found that fast, low-ionization emission regions (FLIERs) are characterized by equal and opposite Doppler shifts of ± 25–200 km s^{-1} with respect to the gas of PNs with which they are associated and in which they seem to be embedded. Here we use the term FLIER to describe those polar knots and jets with anomalous velocities.

FLIERs are of particular interest in the context of the processes by which asymptotic giant branch (AGB) and post-AGB stars shed mass. FLIER morphologies and dynamical ages suggest that nuclei intermittently eject highly collimated mass even as they start blowing a fast and fairly steady wind. FLIERs have not been explored spectroscopically or theoretically in much detail. Such studies are the primary focus of this paper.

The phenomenology of FLIERs bears some elucidation. They appear frequently (20%) in the sample of bright and moderately compact PNs imaged by Balick, preferentially in elliptical PNs whose central stars are too cool, i.e., young, to doubly ionize much He. There is no corresponding emission from any line of moderate- to high-ionization species such as O^{++} or Ne^{++}. In some cases, notably NGC 3242 and NGC 6826, no permitted lines whatsoever are detectable from bright FLIERs.

The dynamical ages of many of the best-studied FLIERs are relatively low—on the order of 1000 yr. Therefore, they were formed during recent periods of rapid stellar evolution and strong mass loss. The dynamical ages of these FLIERs are lower than those of the rims, shells, and halos of the parent PNs. Consequently, the formation of FLIERs may be the result of major instabilities in the mechanism that produces fast stellar winds.

FLIERs are associated with PNs of a wide range of ages. IR images of some proto-PNs suggest that FLIERs may be formed even before the nucleus ionizes the nebula (e.g., Morris & Reipurth 1990). In addition, recent deep imaging studies show evidence of FLIERs at relatively large distances from the nuclei of larger, more evolved PNs, NGC 6751 (Chu et al. 1991) and NGC 6905 (Cuesta, Phillips, & Mampaso 1993). Some PNs, e.g., Fg 1 (López, Roth, & Tapia 1993) and NGC 5189, have multiple pairs of FLIERs on different axes which intersect at the nucleus.

Aside from issues related to the process of stellar mass ejection, the puzzles posed by FLIERs are their high degrees of collimation and supersonic speeds. To this end a detailed study of the spectroscopic properties of FLIERs is relevant, for it can provide clues to the present physical and chemical state of the gas and, indirectly, to the processes by which the gas is excited and shaped. Issues such as these are the focus of this paper.

FLIERs in PNs are not without phenomenological precedent. Specifically, many Herbig-Haro (HH) objects exhibit very similar morphologies, kinematics, and emission-line spectra. HH objects are primarily heated and excited by collisions. Peimbert, Sarmiento, & Fierro (1991) find that shock excitation also affects the spectra of PNs. We shall return to this point later.

FLIERs are just one example of microscopic ($\approx 1''$) structures within PNs. Other examples include rims, various types of knots, and sharp edges of shells and halos. Most previous spectroscopic studies of PNs have used large apertures and, hence, blend the light from the small structures with that of the

background emission. However, the "microstructures" are resolved in the long, narrow slit used for the present observations. Physical conditions in the microstructures are a secondary focus of the present paper.

Hereafter we shall use the following abbreviations, some of which are not standard: [O III] = [O III] λ4959, [N II] = [N II] λ6583, [O II] = [O II] λ3727, [S II] = [S II] λλ6717 + 6731, and [O I] = [O I] λ6300, respectively. The subscripts "aur" and "neb" are used to represent the sum of all optical auroral and nebular line intensities, respectively, e.g., $[S\ II]_{aur}$ = [S II] λλ4068 + 4076 and $[S\ II]_{neb}$ = [S II] λλ6717 + 6731. "Low-(high-) ionization" is abbreviated as L.I. (H.I.); such regions are characterized by the dominance of He^0 (He^+ and/or He^{++}) within the PN's H II region.

2. OBSERVATIONS

The observations were conducted using the Palomar 200 inch (5.1 m) telescope and double spectrograph on the nights of 1990 December 12–14. Standard gratings and spectrograph configurations were used to obtain two simultaneous spectra in the blue (3500–5300 Å) and red (5100–7500 Å). The dispersion is 2.1 Å $pixel^{-1}$ in the blue and 3.1 Å $pixel^{-1}$ in the red, and the effective resolution of the spectrograph is about 2 pixels, or close to 300 km s^{-1}. Along the slit each pixel is 0.″58 for the red camera and 0.″78 for the blue camera.

The seeing averaged 1.″5 for the present observations. The weather was extremely variable, and the transparency changed from poor to excellent during exposures (typically 3–1000 s) lasting more than a few minutes. For these reasons we endeavor to present only relative line intensities measured along the 1″ wide, 2′ long slit.

Data were calibrated using standard IRAF procedures. However, after a careful inspection of the data, we feel that the color calibration of the data is poor, meaning that lines separated by ≥1000 Å may have relative intensity calibration errors of 15% or more. The primary symptom of the color calibration problem is that no self-consistent solution for reddening is obtainable. For this reason our discussions of quantitative line ratios focus primarily on lines found within ≈1000 Å of one another. For other lines we sometimes renormalize to pairs of nearby Balmer lines assumed to be in their unreddened ratios. Reasons for the poor calibration are not understood, and may be related to atmospheric dispersion which may cause the blue light from the flux-calibration stars to fall outside the slit of the spectrograph.

Multiple exposures of the same duration were taken. These were added after unique features such as cosmic-ray hits were removed. The summed exposures were compared in order to identify emission features that might have saturated or partially saturated the detector. Such features were ignored. By using effective exposure times between 3 and 1000 s, we measured the relative fluxes of very bright lines, such as Hα and [O III], and much fainter lines such as [N II] λ5755 and $[Cl\ III]_{neb}$. To correct for erratic transparency, the various spectra were renormalized to a common flux density at 4200 or 6100 Å, as appropriate.

The detector suffers from nonlinearities at very low light levels caused by "sticky" electrons which are not removed from pixels in one read cycle. These electrons are detected, but not always in the proper pixel. In effect, faint features have small tails in the wavelength direction unless the pixel initially contained at least 200 electrons. Bright lunar or nebular continuum, when available, greatly reduces the problem by "preflashing" each pixel. Nonetheless, some data are adversely affected. Generally we are able to recognize affected lines and make first-order corrections when measuring intensities. Given the quality of the sky, more extensive efforts are not warranted.

We report observations of the PNs NGC 3242, NGC 7662, and IC 2149. In each case the spectrograph slit was oriented to include a pair of FLIERs on opposite sides of the central star.

Continuum emission was treated as part of the background and removed. "Slit brightness profiles" (one-dimensional plots of line emissivity as a function of slit position) and the spectra of specific features were extracted. As a check, slit brightness profiles were compared with one-dimensional slices extracted from continuum-contaminated CCD images of the same nebulae in the same position angle obtained by Balick (1987). The agreement was excellent in view of continuum contamination of the images and seeing differences in the two sets of observations.

Owing to the quantity of information and detail, it is convenient to organize the subsequent discussion around the results for individual nebulae. The important conclusions will be synthesized and summarized in the last section of the paper.

3. NGC 3242

BPI consider NGC 3242 to be the prototypical elliptical PN. Morphologically similar PNs include NGC 40, NGC 2610, NGC 6826, NGC 7009, NGC 7354, and NGC 7662, some of which are known to contain FLIERs. Our exposures were made for 3, 100, and 500 s during an hour of unusually clear weather.

Figure 1 shows the nebula, the FLIERs (identified as "knots" in the figure), and the orientation of the slit. The FLIERs are seen in projection on the nebular shell. Of course the FLIERs could actually lie in the PN halo. (Note: Soker, Zucker, & Balick 1992 derive an inclination angle of 70°, whereas BPI estimate the angle to be 30°. In the former case the FLIERs lie outside the nebular shell.)

Where appropriate below, we shall compare our measurements of NGC 3242 with those of Barker (1985), who used a relatively large (3.″4) aperture in five locations in the nebula. His positions 2, 3, and 4 lie close to our slit in the core, in the shoulder, and near the northwest FLIER.

3.1. *Spatial Emission Distribution*

The slit brightness profiles of various emission lines are shown in Figure 2. The profiles are extracted from exposures of various durations in which the lines are not saturated.

First compare the profiles of permitted lines. As expected, all recombination lines from the same species (e.g., H^+, He^+, He^{++}) give indistinguishable results. There is a shoulder of emission which connects the FLIERs to the rim of the nebula (see Fig. 1). As found by Frank, Balick, & Riley (1990), the intensity of the shoulder drops linearly with radius in the recombination lines of H^+ and He^+. The shoulder is not seen in recombination lines of He^{++}, presumably because photons that can ionize He^+ are absorbed in the bright rim of NGC 3242.

Next consider the L.I. forbidden-line distribution along the slit. The FLIERs are particularly prominent in all lines of [O I], [N II], and [O II]. The FLIERs are relatively inconspicuous in the $[S\ II]_{neb}$ lines, consistent with partial collisional quenching expected at densities above above 10^3 cm^{-3}.

Because the FLIERs are conspicuous in the $[S\ II]_{neb}$ lines, the absence of any brightness peak in the [S II] auroral line

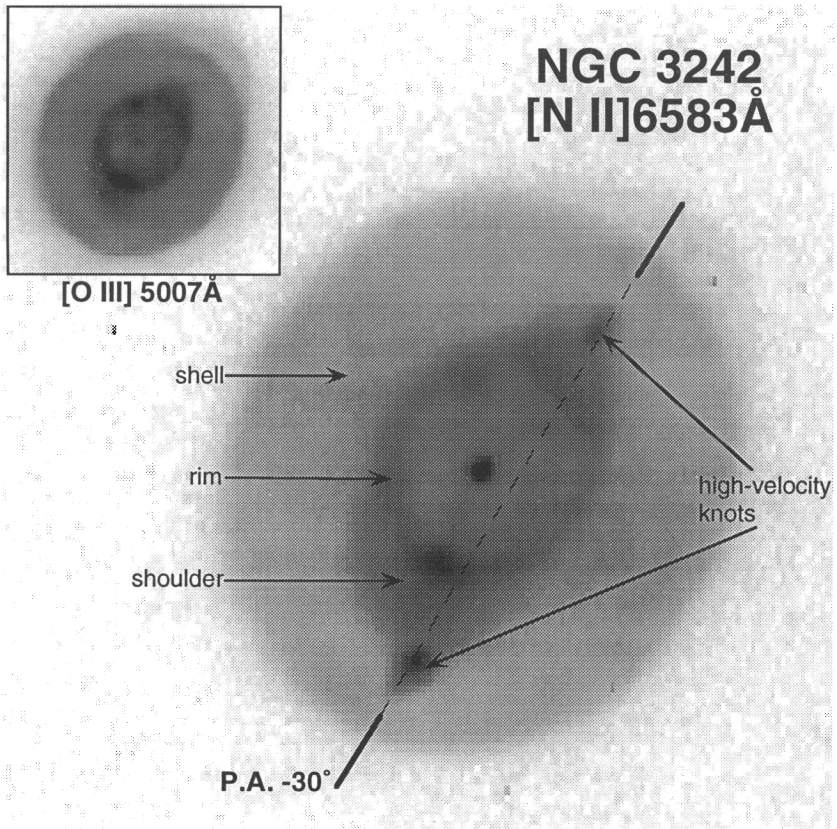

FIG. 1.—CCD images of NGC 3242 in the light of [N II] and [O III] (*inset*) from Balick (1987). North is at the top. The field of view of the [N II] image is 72″. The [O III] subimage is reproduced at about $\frac{1}{2}$ scale. Key morphological components are identified, and the location of the slit is shown. FLIERs are labeled as "knots."

blend at 4072 Å at the location of the FLIERs is puzzling. The absence of FLIER-related $[S\ II]_{aur}$ lines cannot be reasonably explained by abundance or ionization effects. As we show below, density or temperature variations cannot account for the absence of $[S\ II]_{aur}$ lines either. Indeed, the appearance of the $[S\ II]_{aur}$ slit profile is the same as that of the permitted and H.I. forbidden lines. Additionally, the calibrated data show that $0.5 \leq [S\ II]_{aur}/[S\ II]_{neb} \leq 5$ throughout the bright parts of the nebula, which is entirely implausible at any density (see Aller 1984, Fig. 5.11). Barker found the same surprising $[S\ II]_{aur}/[S\ II]_{neb}$ ratios in his spectra.

Perhaps the 4072 Å line is contaminated by C III λ4070 or, more speculatively, [Fe V] λ4071. In any case, the issue of the intensity of the 4072 Å line requires clarification with more suitable, higher dispersion data in the future. We ignore the $[S\ II]_{aur}$ lines hereafter.

Next consider the H.I. forbidden-line distributions of Figure 2. All of these follow the intensity patterns seen in the permitted lines of H^+ and He^+, as expected. There is a possible hint of profile peaks near the FLIERs in the profiles of S^{++} and Cl^{++}.

3.2. *Spectral Characteristics*

We turn next to the spectral characteristics of the rim, knot (i.e., FLIER), shell, and halo. The data measured in the southeast part of the nebula (containing the brightest FLIER) are shown in Figure 3 in logarithmic form because the dynamic range of the data is too great for a linear display. No attempt to subtract the nebular background adjacent to the FLIER has been made in preparing this figure.

Note that an emission line appears in the spectrum of the FLIER near 4571 Å. We tentatively identify it as Mg I] for lack of a reasonable alternative. The same line appears in the spectra of some bright L.I. PNs (L. H. Aller 1992, private communication).

Aside from the L.I. lines, the spectra of Figure 3 are all very similar in shape. (Note: this result is already obvious from Fig. 2.) This reflects the global importance of stellar UV radiation in the excitation of the nebula. But this apparent spectral similarity hides an extremely interesting result.

We have attempted to untangle the intrinsic spectrum of the southeast FLIER from the adjacent nebula on which it is superposed. In principle, we can treat the adjacent nebula as background and subtract it. In practice, the complex structure of the nebula near the FLIERs injects considerable subjectivity into the method. We used two techniques. The spectra of the adjacent shell and shoulder were scaled in such a way that their nebular continuum intensities matched that of the FLIER. These spectra were then subtracted from the spectrum of the FLIER. Additionally, the scaling was performed using an unsaturated He^+ permitted line.

Both methods of removing the background achieve essentially the same result: all of the unsaturated permitted lines vanish. Also, a faint line near 7280 Å appears. This line might be [Ca II] λ7291, whose fainter counterpart at 7323 Å is blended with several $[O\ II]_{aur}$ lines.

The important result is this: FLIERs in NGC 3242 appear to emit no detectable permitted lines or H.I. forbidden lines. Careful inspection of the lower two panels of Figure 2 shows no trace of the FLIERs. Locally, the L.I. lines become very

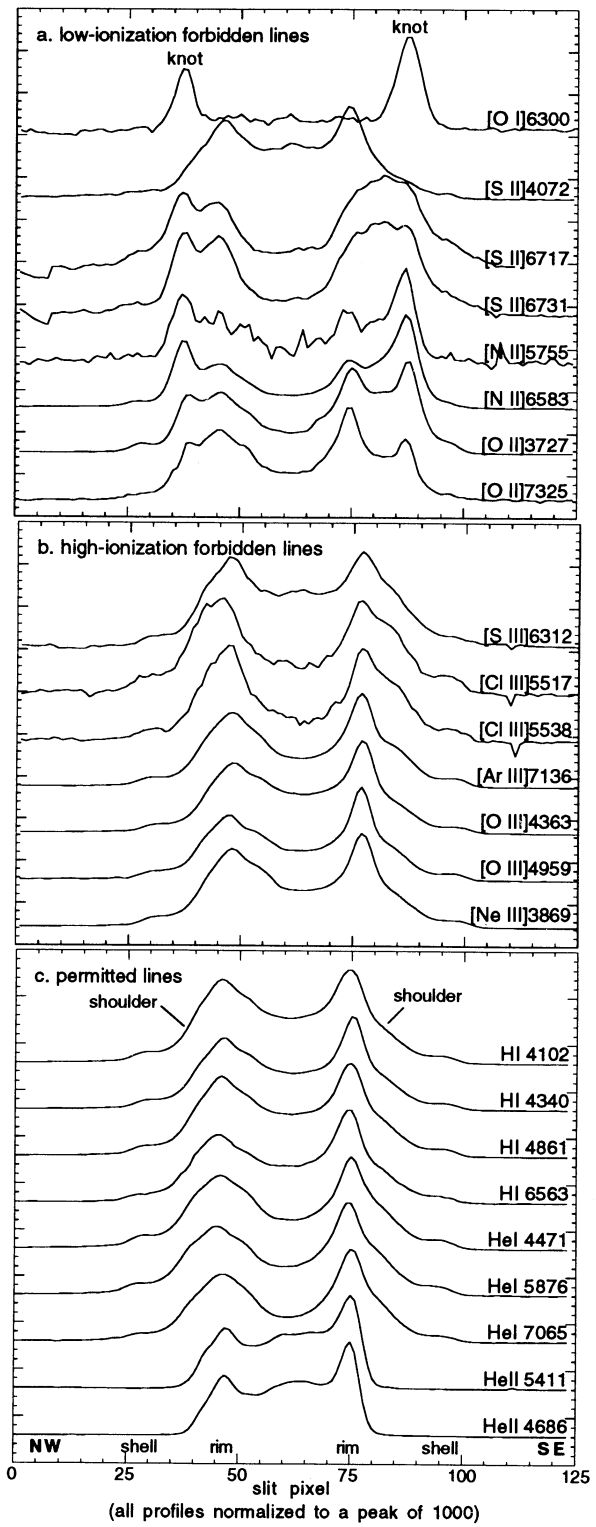

FIG. 2.—Intensity distribution in various emission lines along the slit, from northwest to southeast, for NGC 3242 (P.A. 330°). The abscissa is pixel number at a scale of 1".33/pixel. The continuum has been subtracted, including that of the nucleus. Lines within each subpanel are arranged according to the energy required to make the emitting species by ionization. Key morphological components along the slit are identified; FLIERs are labeled as "knots."

strong near the FLIER, whereas the trends in intensity of other lines show no trace of the FLIERs. The same sort of behavior is seen in the deep CCD images (Fig. 1) and the high-dispersion echelle observations of BPI.

Of course, the FLIERs are faint relative to the nebulae around them. How significant is the limit of permitted line emission? Careful inspection of all available data, including the long-slit echelle observations of BPI in which the FLIERs are spectrally resolved in [N II], enables us assert that Hα is enhanced by no more than 5% near the FLIER. More important, the intensity of the Hα line in the FLIERs does not exceed the intensity of the [N II] forbidden line, i.e., [N II]/Hα > 1. Ratios such as this are not at all characteristic of photoionized nebulae. The significance of this curious result is discussed in more detail after other results are presented.

3.3. *Quantitative Results*

These are presented in Figure 4, in which the distributions of various line ratios as a function of slit position are shown. The locations of the FLIERs are obvious from the [N II] lines, and the positions of rims and the shell are clearly seen in the distribution of, say, [O III] lines.

3.4. *Extinction*

Extinction is small in this nebula. Barker finds the extinction coefficient, c, to be 0.15. The Hγ/Hβ line ratio is sensitive to extinction variations. No credible variations are seen, at least not along the slit. However, since the FLIERs are very weak in the permitted lines we cannot estimate their internal extinctions from Figure 4. It will be interesting to determine reddening in the FLIERs using auroral lines arising from a common level in [S II] (or [O II]) in the future.

3.5. *Global Ionization*

Ionization is commonly characterized by the ionization fraction of the ionization species of He. These fractions can be expressed as $n(\mathrm{He}^{i+})/n(\mathrm{He}) \equiv \mathrm{He}^{i+}/\mathrm{He} = (\mathrm{He}^{i+}/\mathrm{H}^{+}) \times (\mathrm{H}^{+}/\mathrm{H}) \times (\mathrm{H}/\mathrm{He})$, where n is the local density, $i = 0, 1, 2$, $\mathrm{H}^{+}/\mathrm{H}$ is taken to be unity, and H/He is presumed constant.

Figure 4 shows very obvious anticorrelations in $\mathrm{He}^{+}/\mathrm{H}^{+}$ and $\mathrm{He}^{++}/\mathrm{H}^{+}$ along the slit. The sum $(\mathrm{He}^{+} + \mathrm{He}^{++})/\mathrm{H}^{+} \approx \mathrm{He}/\mathrm{H}$ averages 0.09 and is approximately constant (variations of 0.02 from one end of the slit to the other are probably not real). Considering the relevant projection effects, it seems likely that all He atoms in the rims and core are doubly ionized. Aside from the FLIERs, from which no lines of H or He are detected, He elsewhere in the nebula should be entirely singly ionized. The present results are largely in excellent agreement with Barker's.

3.6. *Density*

Densities in the L.I. and H.I. zones are best characterized by $n(\mathrm{S}^{+})$ and $n(\mathrm{Cl}^{++})$, respectively. These are measured from the relative intensities of the pair of $[\mathrm{S\ II}]_{\mathrm{neb}}$ and $[\mathrm{Cl\ III}]_{\mathrm{neb}}$ lines, as presented in Figure 4. The analysis procedures of Aller (1984) were used.

The ratios of the Cl^{++} lines show that the rim is typified by higher densities (6000 cm^{-3}) than is the shell (2000 cm^{-3}). (The actual contrast will be greater because of the sky projection of the shell onto the higher density rim.) Outside the shell the density drops and the Cl^{++} lines become weak. In the halo the $n(\mathrm{Cl}^{++})$ approaches the low-density limit of $\approx 100\ \mathrm{cm}^{-3}$.

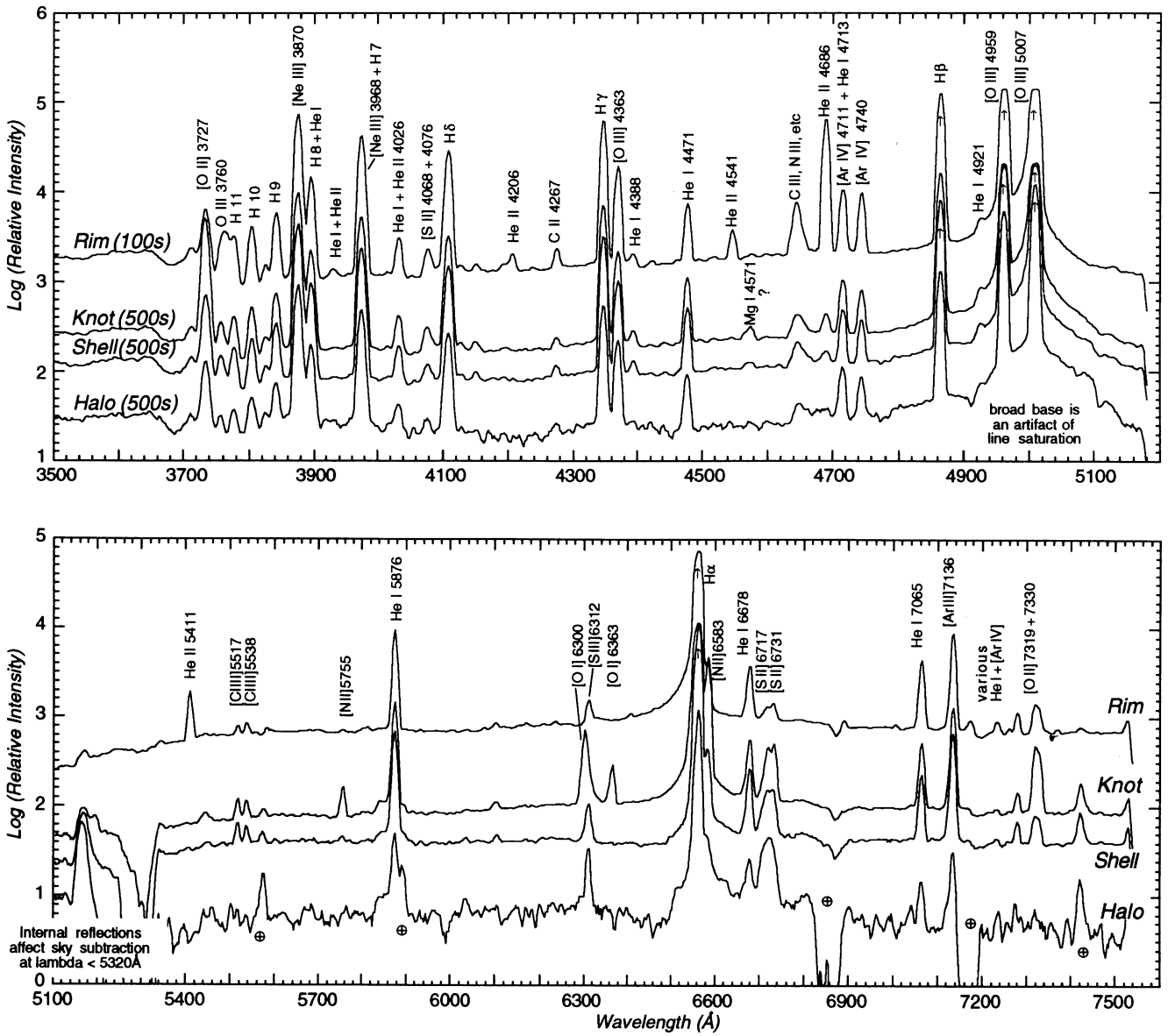

FIG. 3.—Spectra of selected morphological components ("features") of NGC 3242, displayed as the logarithm of the intensity. These spectra are formed by averaging the brightest columns in the CCD data without contaminating the sample with nearby but different features. The name of the feature and the integration time of its spectrum are indicated. A question mark indicates lines with uncertain identifications. FLIERs are labeled as "knots."

The S^+ densities are quantitatively very different from those measured in Cl^{++} lines. This may be partly an ionization effect: We expect the S^+ emission to arise only in the shoulder, shell, and halo, since the gas in the rims is so highly ionized. Unlike $n(Cl^{++})$, $n(S^+)$ does not peak in the rims, which underscores this explanation.

We derive a density $n(S^+) \approx 500$ cm^{-3}—a factor of 4 less than $n(Cl^{++})$ beyond the rims. The disparity in densities is not so easily explained. A similar Cl^{++}–S^+ density discrepancy was noted in HGC 2440 by Richer, McCall, & Martin (1991, hereafter RMM). They atrribute the discrepancy to poorly known Cl^{++} atomic constants.

One might expect the FLIERs to be denser than their surroundings, owing to the locally high surface brightness. But this does not appear to be the case. The FLIERs emit strong [S II] lines; yet, surprisingly, $n(S^+)$ does not increase at the location of the FLIERs. Rather, the brightness of the FLIERs is more likely a marked decrease of ionization without an enhancement of density—or temperature, for that matter (see below). In the halo the density measured from the S^+ line ratio reaches its low-density limit of 100 cm^{-3} or less.

Barker measured intensity-weighted average densities from the [Ar IV] $\lambda\lambda 4711 + 4740$ and $[S\ II]_{neb}$ lines, but not $[Cl\ III]_{neb}$. His results are somewhat uncertain owing to poor signal-to-noise ratio. The values of $n(Ar^{3+})$ drop by about a factor of 2 from about 5000 cm^{-3} in the core and rims to the nebular shell and shoulder. The agreement with our densities measured from the [Cl III] lines is excellent, probably fortuitously. Barker's S^+ densities, which he deems to be uncertain, range from 2100 to 950 cm^{-3} from shoulder to FLIER, whereas our better data indicate 500 cm^{-3} throughout the region. The disagreement is not resolved.

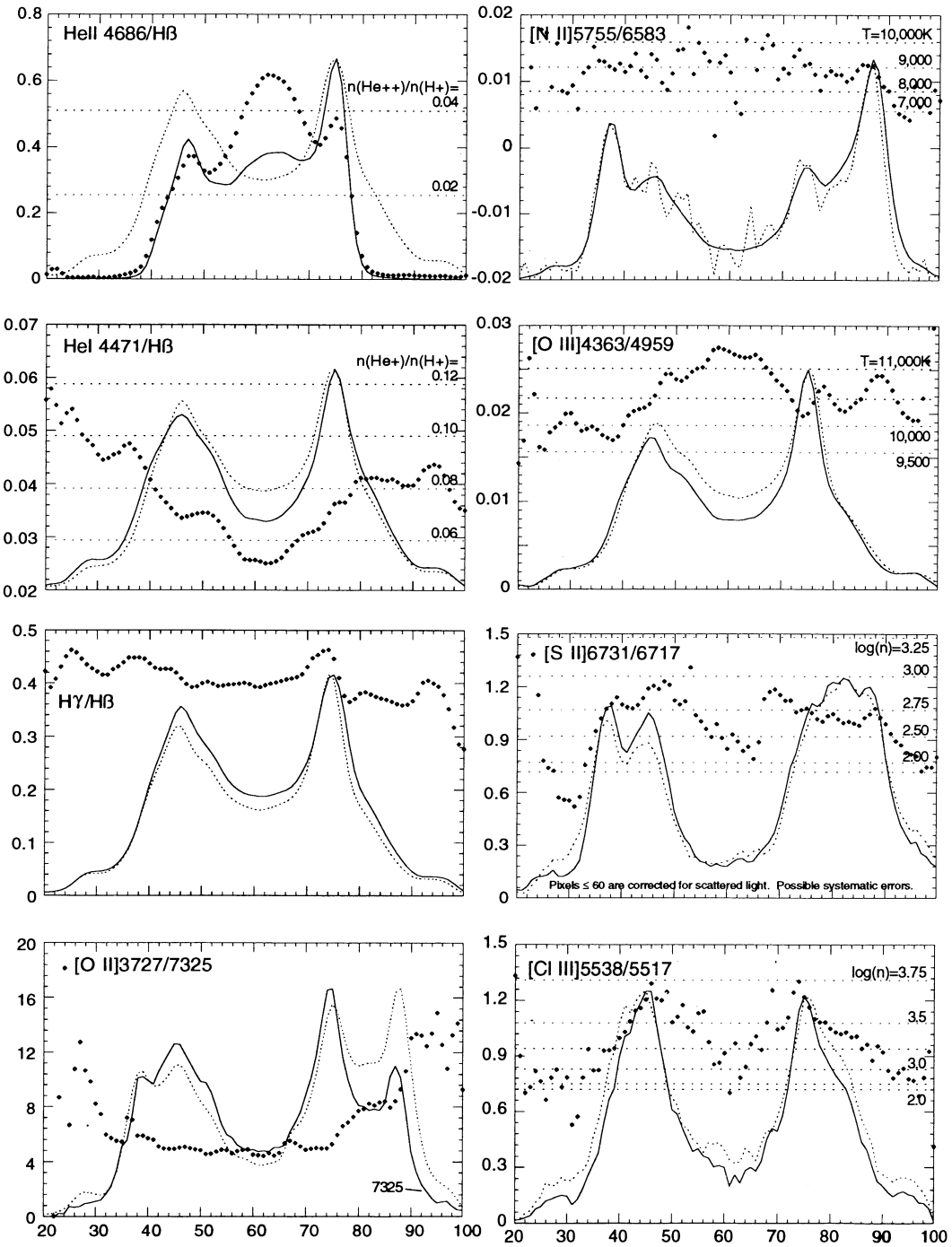

FIG. 4.—Line ratios (*dots*) and the normalized slit profiles of the emission lines from which the ratio is formed (*solid and dashed lines*), plotted as a function of slit position (i.e., pixel number) for NGC 3242. Profile normalization is arbitrary and intended only for clarity. The scale of the abscissa is described in Fig. 2. Horizontal dotted lines are used to indicate the relationship between line ratio and a physical property of the nebula such as ionic abundance, density, or temperature. See text for other details

3.7. *Temperature*

Temperatures in the L.I. and H.I. regions are measured by the [N II] and [O III] lines, $T(N^+)$ and $T(O^{++})$, respectively. $T(N^+)$ is constant at about 9000 K throughout all regions where the lines are sufficiently bright to measure temperatures, including the FLIERs. In the rim the temperature seems to be somewhat higher, $T(O^{++}) \approx 11{,}000$ K, than elsewhere, $T(O^{++}) \leq 10\,000$ K. These values are in good agreement with Barker's.

We caution that our absolute temperatures may be in error by $\approx 10\%$ owing to the problems with the color calibration, as noted earlier. Therefore, the agreement with Barker's temperatures may be fortuitous. In any case, our measured temperature variations along the slit are real.

3.8. *Miscellaneous*

Another potentially interesting diagnostic line ratio is $[O\ II]_{neb}/[O\ II]_{aur}$. This ratio is sensitive to both density and temperature (Aller 1984, Fig. 5.10). There are substantial variations in the ratio between 5 and 12 along the slit (Fig. 4). In view of the lack of major variations in either $n(S^+)$ or $T(N^+)$ along the slit, the huge variations in the density- and temperature-sensitive $[O\ II]_{neb}/[O\ II]_{aur}$ ratio is unexpected. Moreover, values between 5 and 12 are not at all physically reasonable. We leave resolution of this quandary to the future.

The actual value of the $[O\ II]_{neb}/[O\ II]_{aur}$ ratio between 5 and 12 casts aspersions on the validity of the data. These values are not within the range of any physically reasonable values. This could be the result of a very poor flux calibration (the two sets of lines lie at opposite ends of different spectra), in which case the variations along the slit are still significant. Perhaps the resolution to the quandary lies in the contamination of the auroral [O II] lines by nearby [Ca II] or other emission lines.

3.9. *Discussion*

The results of the line-ratio analysis suggest that, compared with the regions around them, FLIERs are much lower in ionization, higher in velocity, and about the same in density and temperature. We reach an apparent dilemma: how can the FLIERs, on the one hand, and the adjacent shell and shoulder, on the other—regions of the same density and temperature, and subjected to much the same stellar radiation—vary so dramatically in their ionization states?

Two plausible hypotheses are that the observed emission from the FLIERs is associated with either an ionization front (IF) or a shock. We will explore the veracity of these hunches from several directions: by consideration of morphology, kinematics, and spectral information and by analogy to other types of similar regions.

3.10. *IF Models*

Most IFs appear filamentary and narrowest in their radial dimension. In order to reconcile the small transverse size of the FLIERs with an IF model, we can make the ad hoc assumption that the observed L.I. lines arise on the starlight-bathed, backward-facing side of a small dense blob of neutral gas. There will, of course, be spatial offsets in the locations of the [O I], [S II], and [N II] lines, although the differences might not be observable if the IF is very thin, i.e., $\leq 1''$. Let us assume the PN to be at a distance of 1 kpc (see Acker et al. 1992). Then, if the thickness of the IF is the mean free path of a 40 eV photon whose dimensions correspond to $1''$, we require that $n(H^\circ) > 300\ cm^{-3}$. This is within range of the observed densities. The IF model just passes the first test.

The speeds of the FLIERs are $\pm 25\ km\ s^{-1}$ with respect to the gas that surrounds them, or more if projection effects are significant. However, flow velocities through an IF are limited to the sound speed, $\approx 10\ km\ s^{-1}$. Moreover, the absence of an observed pressure gradient and edge-on projection suggest that the flow velocities should be even smaller than this. Hence the observed kinematics in which FLIERs have redshifts of $\geq 25\ km\ s^{-1}$ with respect to their local surroundings are difficult to reconcile with an IF interpretation for the FLIERs.

As for the spectral properties expected from an IF, detailed predictions are impossible without knowledge of the density and temperature in the neutral gas outside the IF. Computations predict an enhanced density in the IF, which is not observed. Also, H^+ recombination lines should be detectable. No clear evidence of such lines is seen. The lack of a rise in temperature through the IF is consistent with recent model calculations (RMM).

3.11. *Shock-Excitation Models*

The spectral character of FLIERs is reminiscent of shock-excited nebulae such as HH objects. Aside from [Fe II] and [Fe III] lines, a comparison of the identified FLIER's L.I. forbidden lines with those of HH 1 measured by Solf, Böhm, & Raga (1988, Table 1) shows nearly one-to-one correspondence. Although the line ratios differ in detail, the same lines are prominent in both spectra. (The presence of iron lines in the HH object can be explained by its much higher densities.)

Are FLIERs phenomenological counterparts of HH objects? A very popular model for HH objects is that they are the result of bow shocks attached to outward-flowing "bullets" or streams of dense gas (Noriega-Crespo, Böhm, & Raga 1992, 1989; Blondin, Königl, & Fryxell 1989; Hartigan 1989; Hartigan, Raymond, & Hartmann 1987, hereafter HRH). The brightest emission arises in the stagnation zone upstream in which the effective collision speed is the greatest. Let us explore this model further.

The analogy with HH objects argues that shocks associated with bullets or jets might be collisionally exciting the L.I. lines in FLIERs. Certainly the morphologies of FLIERs resemble bow shocks associated with small, fast-moving neutral bullets. Moreover, the observed shoulders could be formed as gas compressed or entrained in the tails of the bow shocks becomes ionized by direct stellar UV photons. So the model easily passes the morphology test.

Consider the kinematics. After correction for inclination effects, the true space velocity of the FLIERs is probably 50–70 $km\ s^{-1}$. At these velocities shock models predict that L.I. forbidden lines will be strong, whereas H.I. forbidden lines are relatively weak (e.g., HRH). In other words, the shock-excitation model nicely relates the observed spectral character to the kinematics of the FLIERs, at least qualitatively.

However, on a more sobering note, all shock models that might account for bright L.I. forbidden lines *always* predict $H\alpha > [N\ II]$ (see HRH). The FLIERs in NGC 3242 exhibit the reverse behavior. To rescue the model, we can hypothesize that FLIERs are enriched in N, O, and perhaps other elements relative to H and He. Unfortunately, this interesting but highly speculative hypothesis is untestable with the present data set. These data are not conclusive.

The bow-shock model also requires a large pressure gradient. In the model the brightest emission arises in the stagnation region. Here the pressure is given by the ram pressure imposed by the upstream gas. The gas in the stagnation region becomes compressed. In the steady state the gas becomes hot in the shock, recombines, and cools efficiently through radiation. Its pressure is large compared with the medium downstream. Finally, the measured FLIER density, $n(S^+) \approx 500\ cm^{-3}$ is very low compared with the densities generally assumed for interpretive models. Nonetheless, the shock model survives.

The largest problem for the shock model is an obvious one. Stellar radiation should be permeating the shock, causing considerable preionization. At densities of $500\ cm^{-3}$ the recombination time is about 2000 yr, and during this time the preionized gas leaves the recombination zone downstream of the shock before it can recombine to low-ionization states.

Thus the very low ionization of the FLIERs, one of their defining characteristics, is not in accord with the model unless the shock is somehow shielded from the stellar UV photons.

In summary, the present observations of NGC 3242 are not explained well by either the shock or the IF model. Given this situation, any estimate of the chemical abundances in the FLIERs is likely to be erroneous.

4. NGC 7662

NGC 3242 and 7662 are very similar in their overall morphological and kinematic properties. Both PNs are elliptical, both have rims, both have shells with highest brightness along the equatorial (i.e., minor) axis, and both have bright FLIERs.

[N II] and [O III] images of NGC 7662 are shown in Figure 5. Unlike NGC 3242, the FLIERs of NGC 7662 are seen in projection outside the shell on the faint nebular halo. In addition to the bona fide FLIERs, NGC 7662 has several low-velocity, low-ionization knots along the outer perimeter of the shell, whereas NGC 3242 does not. However, these knots have neither the velocities nor the symmetric distribution to be classified as FLIERs, and we ignore them below.

The nebula was observed in two slit positions. We describe the results for the slit in P.A. 22°. The slit passes through both FLIERs (designated "high-velocity knots" in the figure). The data in P.A. 6° follow a faint filament of high-velocity emission from the southernmost part of the rim into the southern FLIER. These data, observed in variable cloudiness, do not turn out to be particularly interesting and are not described further here.

We obtained one 3 s and three 300 s integrations, mostly in clear weather. A few emission lines are very faint in the short exposure but nearly saturate the longer exposures. These lines include the Hβ and He I λ5876 lines for which the peaks (i.e., at the intersection of the slit and the rims) may be affected by very mild saturation. The use of these lines is avoided in the following discussions. Although the [N II] λ6584 line is not saturated in the longer exposures, the nearby Hα line is so heavily saturated that electrons in the relevant pixels have "overflowed" into the pixels of the [N II] line as the electrons were transferred in the CCD.

4.1. *Spatial Emission Distribution*

Figure 6 shows the slit brightness profiles of strong lines after removal of the stellar and nebular continuum. Question marks identify uncertain features. The pixels near the question mark in the [N II] profile are affected by electrons in the badly saturated Hα line, as just noted. The question marks in the [S II] profiles denote regions where reflections within the spectrograph produce ghost images. We feel that the ghost images have been successfully removed and that [S II] features identified with the question marks are credibly, if not accurately, depicted.

The basic trends and conclusions are much the same as in the case of NGC 3242. To review briefly: recombination lines

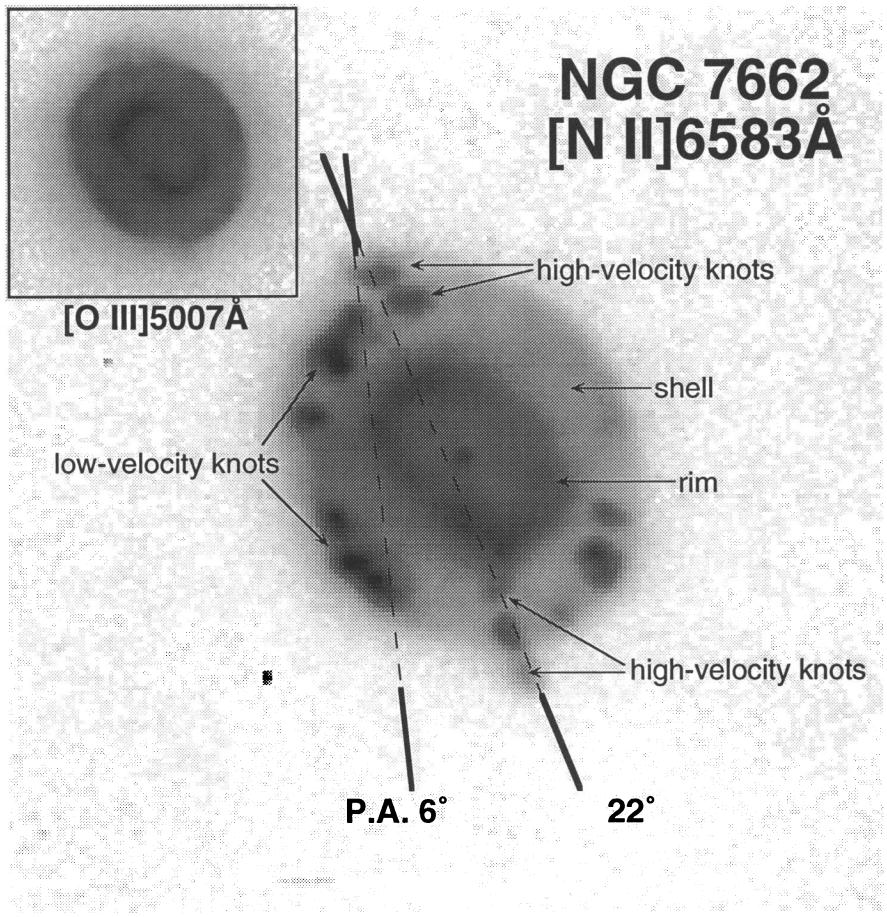

FIG. 5.—CCD images of NGC 7662. See legend to Fig. 1 for other details

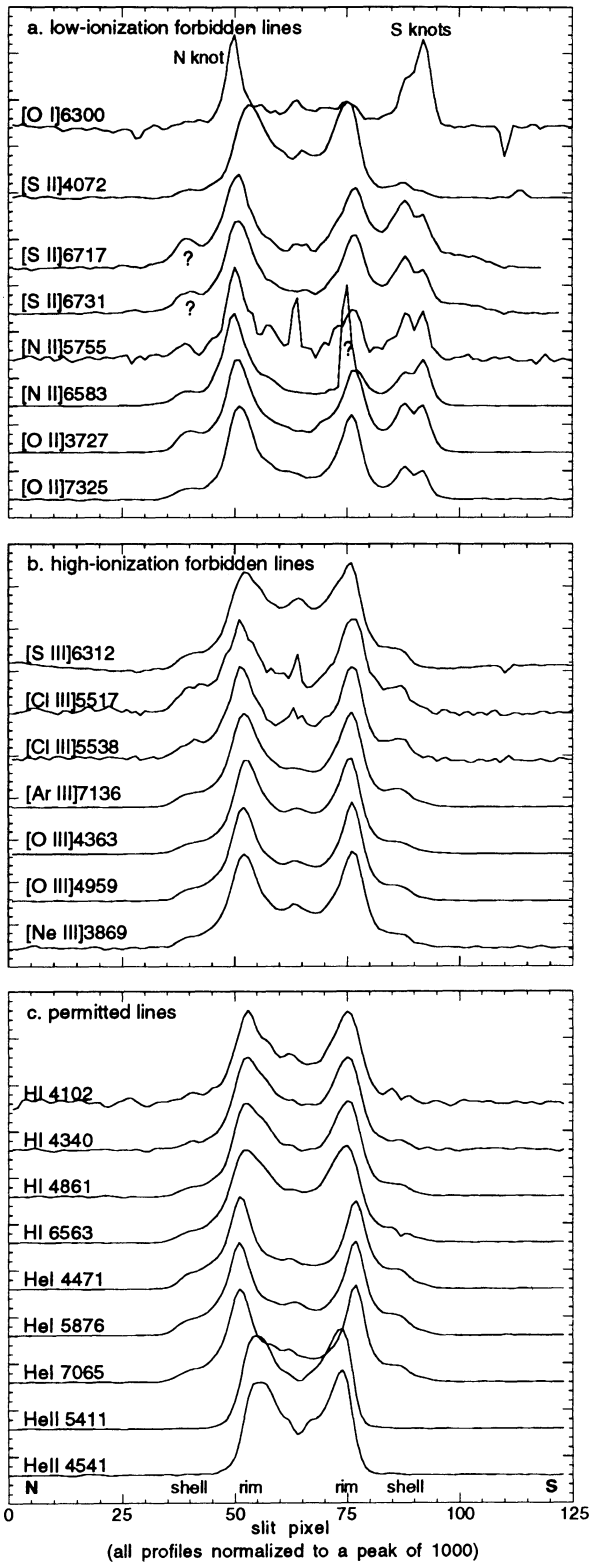

FIG. 6.—Intensity distribution in various emission lines along the slit, from north to south, for NGC 7662 (P.A. = 202°). See legend to Fig. 2 for other details

of H^+ and He^+ are fairly similar in distribution. Recombination lines of He^{++} are limited in extent to the radius of the rim, showing that the nebula is ionization-bounded for photons of energies ≥ 54 eV. The H.I. forbidden-line distribution largely mimics that of the H^+ and He^+ recombination lines, as found for NGC 3242.

FLIERs are very prominent in the L.I. forbidden lines, especially [O I]. There are two FLIERs on the south side of the slit, each with slightly different spectroscopic properties. The innermost of the two has weak counterparts in the H.I. forbidden lines with ionization potentials of the lowest species, i.e., [S III] and [Cl III]. There are also two FLIERs to the north, although the innermost one lies just outside the slit. It is likely that some of the emission from this FLIER is detected. As for NGC 3242, the FLIERs are not seen in an emission line near 4072 Å which we identify as the blended $[S\ II]_{aur}$ lines. All of the problems relating to this line in the context of NGC 3242 apply to NGC 7662 as well.

4.2. *Spectral Characteristics*

The spectra of the rim, a portion of the shell, and the two southern FLIERs are shown in Figure 7. Once again, the major conclusions of NGC 3242 pertain to NGC 7662. For NGC 7662 it is straightforward to disentangle the spectrum of the FLIERs from the relatively faint local background.

Permitted lines, H.I. forbidden lines, and L.I. forbidden lines are all detectable in the spectrum of the FLIER (i.e., "knot") of NGC 7662. Ignoring the L.I. forbidden lines, the lines of the FLIER are in essentially the same ratios as in the nebular shell. It is possible, if not likely, that all of these lines are excited in the same way, presumably by stellar UV photons.

4.3. *Quantitative Results*

These are summarized in Figure 8. We shall compare our results with those of Barker (1986), who measured line ratios through a 3".4 aperture in five positions in NGC 7662. None of his positions lies near our slit of any of the FLIERs, although all but one lie in or near the rim and shell.

The character of L.I. forbidden lines in the FLIER is highly reminiscent of that of the FLIERs in NGC 3242. In contrast to the case of NGC 3242, permitted lines are readily detectable in the FLIERs. Specifically, the Hα/[N II] ratio is on the order of 5 in the south FLIERs of NGC 7662, and even higher in the north FLIER—far greater than in the case of NGC 3242. This result is perfectly acceptable from the point of view of shock excitation theories (e.g., HRH) and photoionization models (e.g., RMM).

4.4. *Extinction*

The extinction appears to be low, although the poor flux calibration renders a quantitative conclusion impossible. Careful measurements of c by Barker range from 0.2 close to the rims to 0.4 in the shell and halo. No local internal variations in extinction are supported by our observations.

4.5. *Global Ionization*

As in NGC 3242, the He^+-He^{++} ionization front is interior to the nebula, although this IF in NGC 7662 is associated with the *interior* portion of the rim. Also as in NGC 3242, there is a clear gradient in the ionization state from inside to outside. The He abundance is about 0.093 in NGC 7662—about the same as in NGC 3242. Barker finds the same general results.

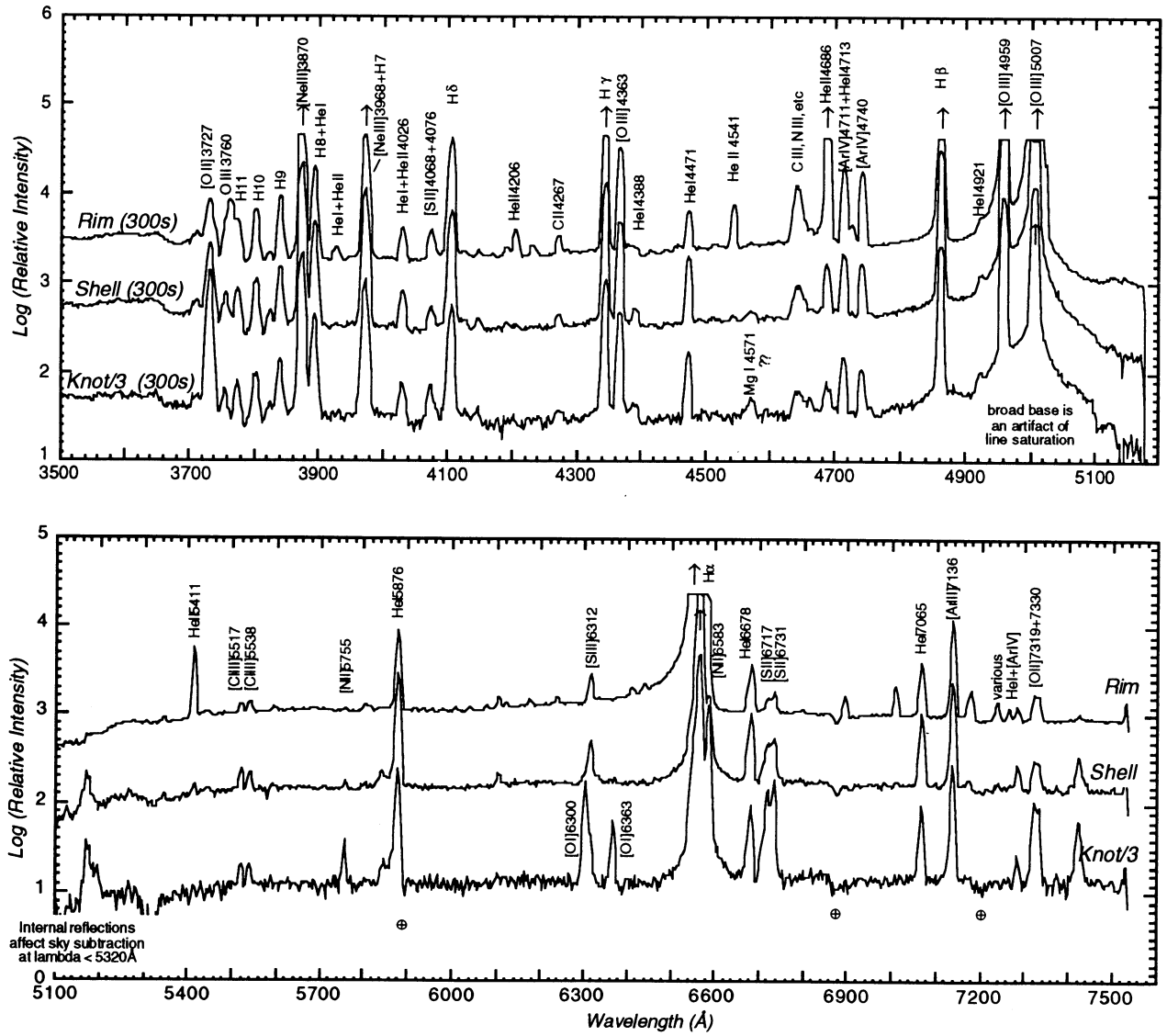

FIG. 7.—Spectra of selected features of NGC 7662. See legend to Fig. 3 for other details.

4.6. *Density*

Both S^+ and Cl^{++} lines arise in the rim and shell. For the rim we find $n(S^+) \approx n(Cl^{++}) \approx 3000\ cm^{-3}$, with a tendency for $n(Cl^{++})$ to give larger values by a factor of 2 [Recall that $n(Cl^{++})/n(S^+)$ is about 4 in those regions of NGC 3242 in which both lines are strong.] The densities appear to be highest between the rims, suggesting that the density estimated above is actually an intensity-weighted average of the rims and portions of the shell which lie along the same line of sight. A crude correction for the projection of the shell onto the rims places the derived densities at or close to the high-density limits of both lines, i.e., $n(S^+) \geq 10^4\ cm^{-3}$ and $n(Cl^{++}) > 10^{4.5}\ cm^{-3}$.

The densities of the shell, halo, and FLIERs are lower than that of the rims. The S^+ lines yield $n \approx 10^3\ cm^{-3}$ both in the FLIERs and in the shell. Although the data are noisy, the $[S\ II]_{neb}$ line ratio suggests a density of about 500 cm^{-3} for the innermost part of the halo near the FLIERs.

Although a close comparison between our measured densities and Barker's is unwarranted owing to sampling differences and the low signal-to-noise ratio of his measurements, his measured densities are generally in accord with ours. Except in the halo, where all lines are weak, he also finds that $n(Cl^{++})/n(S^+) > 1$ whenever both densities can be determined at the same location.

4.7. *Temperature*

$T(O^{++})$ is measured at very high signal-to-noise ratio to be 12,000 K in the shell outside the rims, i.e., the He^+ zone, and 14,000 K in the core, i.e., the He^{++} zone. Projection effects probably cause an underestimate of the actual temperature contrast. The variations in $T(O^{++})$ are almost certainly the result of inefficient cooling in the higher ionization zone which is caused by the ionization of the primary coolants, O^{++} and Ne^{++}. A more detailed discussion can be found in RMM.[1]

[1] The photoionization models of RMM are the most complete and accurate for the L.I. lines. They have produced tables of expected line fluxes for nebulae consisting of a thin shell of solar abundances at various distances from a star at a temperature of 200,000 K. This stellar temperature is about a factor of 3 too large to apply to either HGC 3242 or NGC 7662, but their results are still illustrative for our purposes.

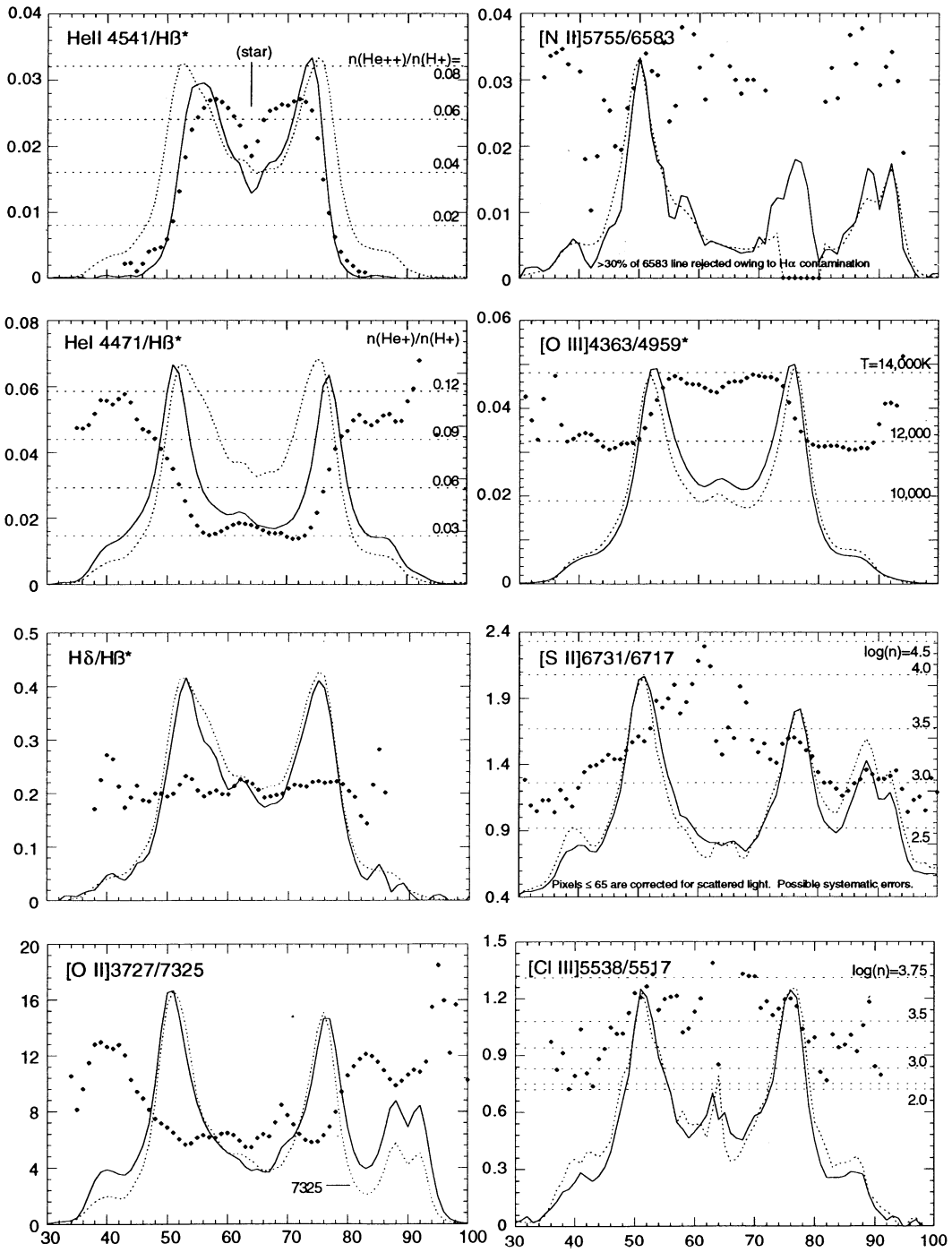

FIG. 8.—Line ratios and normalized slit profiles of the emission lines for NGC 7662. See legend to Fig. 4 and the text for other details.

[O III] emission from the FLIERs is difficult to isolate and, hence, to allow a reliable estimate of their O^{++} temperatures.

Barker finds values and gradients in $T(O^{++})$ in extremely good agreement with ours. His analysis of UV lines of O^{3+} in the core suggest that temperatures sampled by these lines are close to 16,000 K inside the rim and 13,600 K just outside the rim, also in good agreement with the present measurements.

Since the FLIERs are bright in [N II], a determination of $T(N^+)$ would be of considerable interest. Unfortunately, the bright [N II] λ6584 lines has been contaminated by "overflow" electrons from the saturated Hα line nearby, especially where the Hα line is brightest. The problem is most severe along the [N II] line profile edge closest to the Hα line. In extracting the [N II] line profile we had to eliminate two rows of [N II] line data. The net result is that the absolute [N II] line intensity is badly underestimated, and $T(N^+)$ cannot be measured absolutely from our data. Variations in $T(N^+)$ along the slit appear to be small, but any conclusions are limited by the poor signal-to-noise ratio of the [N II] λ5755 line.

Barker measured $T(N^+)$ at only one location at which the aperture covers both halo and portions of a low-velocity L.I. knot north of the star. He finds $T(N^+) = 11{,}000$ K there.

4.8. *Miscellaneous*

We briefly consider the variations of $[O\ II]_{neb}/[O\ II]_{aur}$ along the slit. The same trends seen in NGC 3242 are seen for NGC 7662: the ratio rises from lower values (about 5) in the central regions to ≈ 12 near the FLIERs. Just as in the case of NGC 3242, the measured $[O\ II]_{neb}/[O\ II]_{aur}$ line ratio varies systematically between 5 and 12 and lies outside the range of any reasonable values.

4.9. *Discussion*

To summarize the observational results of the FLIERs of NGC 7662, we find a relatively low-ionization spectrum relative to the rest of the nebula. The permitted lines appear to be prominent in the spectrum of the FLIERs of NGC 7662; e.g., $H\alpha/[N\ II] \geq 5$, whereas the ratio is less than unity for the FLIERs of NGC 3242. The data suggest that the densities of the FLIERs are $\approx 10^3$ cm^{-3}—about the same as those of the nearby shell and about a factor of 2 greater than the adjacent halo. Values of $T(N^+)$ in the FLIERs and shell appear to be about the same, suggesting a mild pressure gradient between the FLIER and its immediate environment.

We now relate the observations of the FLIERs to models that might account for their properties. For this purpose we consider the southernmost FLIER which is most cleanly projected onto the faint nebular halo. Looking at the calibrated data, *and making no attempt to subtract any background*, we find the following line strengths relative to $H\beta$ (=100): $H\alpha = 274$; [O III] = 51; [O II] = 140; [N II] > 50; [S II] = 20; [O I] = 10. However, it is very important to note that the $H\alpha$, $H\beta$, and [O III] lines are dominated by the halo, and not by the FLIERs, as seen in Figures 5 and 6. Indeed, the line profiles of these lines are sharply and nonlinearly decreasing with radius at the position of the FLIERs, whereas the L.I. lines show a distinct maximum. Consequently, the ratios of the L.I. to $H\beta$ lines above are all greatly underestimated. Using a strong FLIER line as a standard for the other lines, we find [O I]/[N II] < 0.2 and [O I]/[SII] = 0.5.

The discussion follows the pattern of that for NGC 3242: we consider thermal- and shock-excitation models in view of the morphologies, kinematics, and spectral properties of the FLIERs in NGC 7662.

Consider first the shock excitation model. As in NGC 3242, the properties of collisionally excited bow-shock models are very nicely consistent with the morphologies, kinematics, and spectra of the FLIERs. BPI show that when they are kinematically separated from the nebula, the FLIERs of NGC 7662 are more filamentary or jetlike than knotty, much like the FLIERs in NGC 6751 and NGC 7354. This morphology is similar to several HH objects. BPI measured Doppler shifts of the FLIERs in NGC 7662 as ± 50 km s^{-1} and an inclination angle of 40°. Consequently, the FLIERs might be expected to be characterized by shocks of ≈ 100 km s^{-1}, which is very close to the velocities estimated by BPI. The spectra expected from such shock-excited regions (HRH) are fully in accord with the observations, so the outflow velocities and spectra are nicely compatible. $H\alpha$ is detected in the FLIERs of NGC 7662 at just about the intensity predicted by HRH models at the appropriate velocities. In short, the arguments of this paragraph are very strong circumstantial support for the shock-excitation model. Indeed, the FLIERs of NGC 7662 could be mistaken for HH objects, were the rest of the nebula absent!

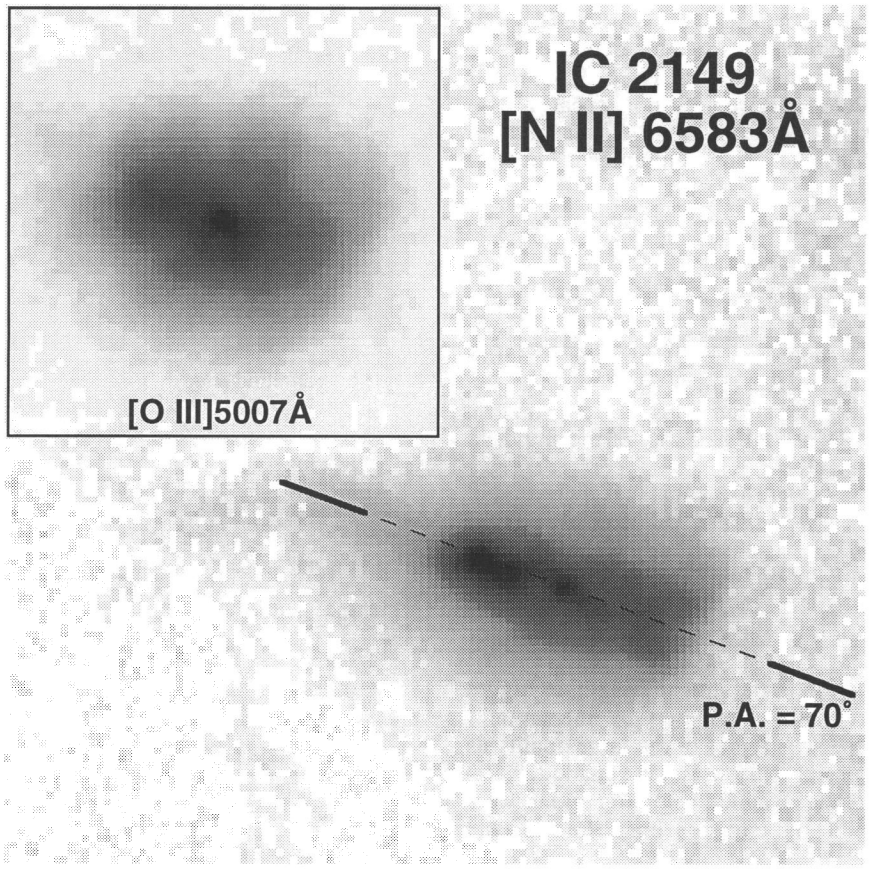

FIG. 9.—CCD images of IC 2149. See legend to Fig. 1 for other details.

The shock model hangs for exactly the same reason as in the case of NGC 3242: the very low ionization of the FLIERs seems inconsistent with the likely large flux of stellar UV photons given the low densities, and attendant long recombination times, that are expected. In this regard, the numerous low-ionization, low-velocity knots around the perimeter of NGC 7662's shell, if they are to be explained as shocked cloudlets, share the same problem as the FLIERs. The shock model is all but ruled out.

Next, consider the photon-heated, thermally excited model for the FLIERs of NGC 7662. These can be divided into two types of hypotheses: (1), dense cloudlets in photoionization equilibrium and (2) an edge-on IF. The two models share many of the same successes (e.g., explanation of line ratios under certain conditions) and failures (e.g., the velocities of the FLIERs are not naturally incorporated) as encountered above for NGC 3242.

Insofar as dense cloudlets are concerned, the observed spectra of the FLIERs of NGC 7662 fit comfortably within the grid of ionization-equilibrium forbidden-line strengths predicted by RMM. On the other hand, if an IF exists, then, like the FLIERs of NGC 3242, the IF must separate ionized nebular gas from a dense neutral cloud of small transverse dimensions.

The ionization-equilibrium cloudlet model fails decisively on morphological grounds. The observations show that the FLIERs are not in pressure equilibrium with the halo in which they are embedded. The higher pressures in the FLIERs should lead to their rapid disintegration on time scales of their sound crossing times. In particular, any dense clouds will expand at 10 km s^{-1} (or more) while moving radially outward at between 50 and 100 km s^{-1} and, hence, should appear much larger than observed.

Consequently, a small, dense, neutral cloud with an IF on its starward side is required to account for the small size of the FLIER. The same discussion presented for NGC 3242 in this context applies to NGC 7662, and we need not repeat it. Also as for NGC 3242, the excitation mechanism is sufficiently in doubt that an estimate of the chemical abundances is not warranted.

5. IC 2149

IC 2149 is a small, high surface brightness PN which has received relatively little attention. Images of IC 2419 are shown in Figure 9. The nebular structure in [N II] is entirely dominated by a small knot east of the central star, whereas the structure in [O III] is much more amorphous. The asymmetric morphology of IC 2149 does not fall into any of the standard categories (elliptical, bipolar, etc.).

The expansion velocity in [O II], 40.3 km s^{-1}, is twice that of [O III] (Gussie & Taylor 1989; Wilson 1950), suggesting that the L.I. knot is characterized by a substantially larger Doppler shift than the remainder of the nebula. Thus the knot has a superficial similarity to FLIERs. For this reason, and because of the advantageous location of the object in the December sky, we observed IC 2419.

The orientation and location of the slit can be seen in Figure 9. The observations were badly hampered by intermittent clouds, and the resulting spectra are not of the same quality as those of the other PNs. Useful exposures were made for 100 and 1000 s. The star and the brighter nebular regions were saturated in all exposures in the emission lines Hα, Hβ, and [O III].

5.1. *Spatial Emission Distribution*

Slit brightness profiles are plotted in Figure 10. Dashed lines indicate regions where removal of the bright stellar continuum is compromised by saturation problems. No lines of He^{++} are detected. The east knot is very conspicuous in all lines except [O III] and [Ne III], especially those of low ionization. This

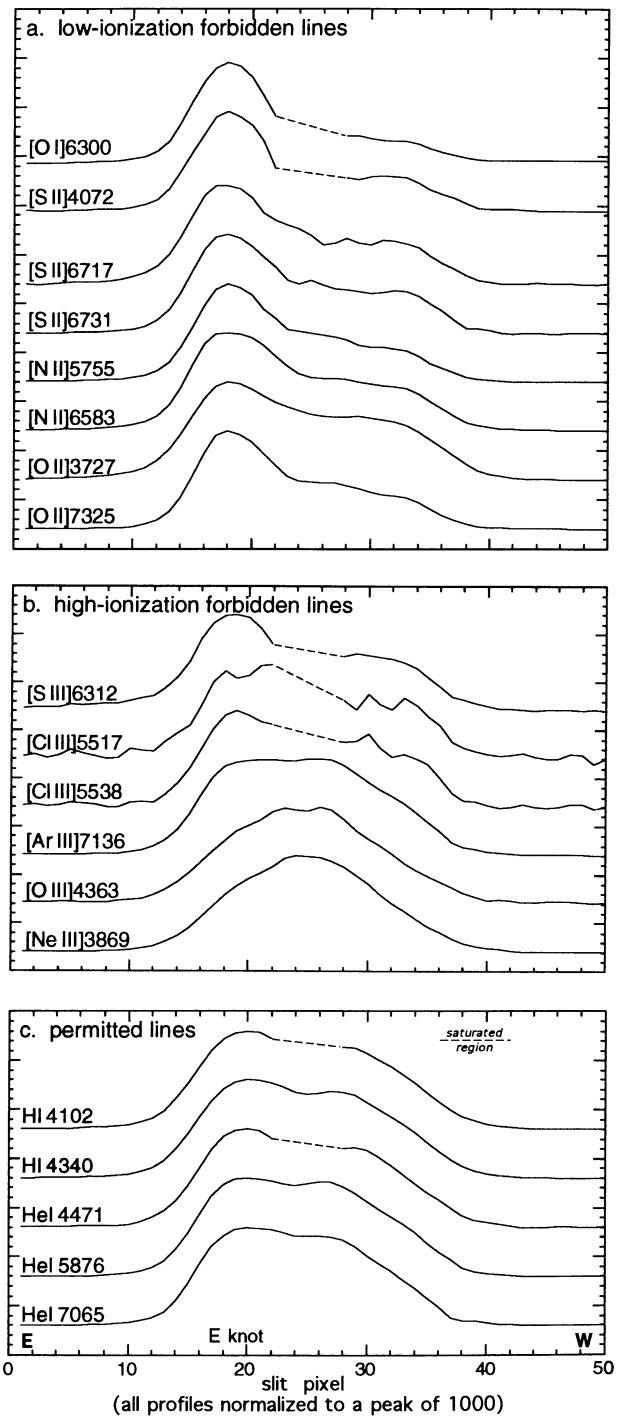

FIG. 10.—Intensity distribution in various emission lines along the slit, from east to west, for IC 2149 (P.A. 70°) Regions in which saturation makes the subtraction of the continuum impossible are shown as dashed lines. See legend to Fig. 2 for other details

suggests that the total stellar production rate of photons above 35 eV is relatively small, and that no stellar photons more energetic than ≈27 eV reach the knot. The east knot could be a recombination region behind a shock.

The [S II] nebular and auroral lines have the same overall distribution along the slit. While this is expected, recall that no such behavior was found for either NGC 3242 or NGC 7662.

5.2. *Spectral Characteristics*

The spectra at three locations in IC 2419 are shown in Figure 11. (The graph of the west nebula was offset by 1 unit for display purposes.) The character of the spectra are similar, except that the L.I. forbidden lines such as [O I] and [N II] are enhanced in the east knot relative to other lines, as we have noted earlier. Many of the remarks made earlier about the spectral character of FLIERs in NGC 3242 and NGC 7662 pertain to the east knot of IC 2419.

5.3. *Quantitative Results*

The distribution of line ratios is shown in Figure 12. Line intensities and their ratios are uncertain near the star (pixel 25) owing to saturation effects. Some of the line-ratio plots made in Figures 4 and 8 were omitted owing to the saturation of Hα, Hβ, and [O III] lines. The remaining H^+ recombination lines lie too close to one another in wavelength to be useful for measuring extinction variations along the slit.

The highlights of Figure 12, which pertain to the brighter regions, are (1) that the He^+/H^+ is uniform and about 0.11; (2) that $T(N^+)$ is about 9000 K and may rise by 10% in the east knot; (3) that $n(S^+)$ is uniform and ≈ 3000 cm^{-3} with no enhancement in the east knot; (4) that $n(Cl^{++}) \approx 2n(S^+)$, as in NGC 7662; (5) that $[S\ II]_{aur}/[S\ II]_{neb} \approx 0.1$, implying a temperature of 9000 K [in excellent agreement with $T(N^+)$]; and (6) that $5 \leq [O\ II]_{neb}/[O\ II]_{aur} \leq 12$ with the same caveats regarding possible line contamination, and the same trends

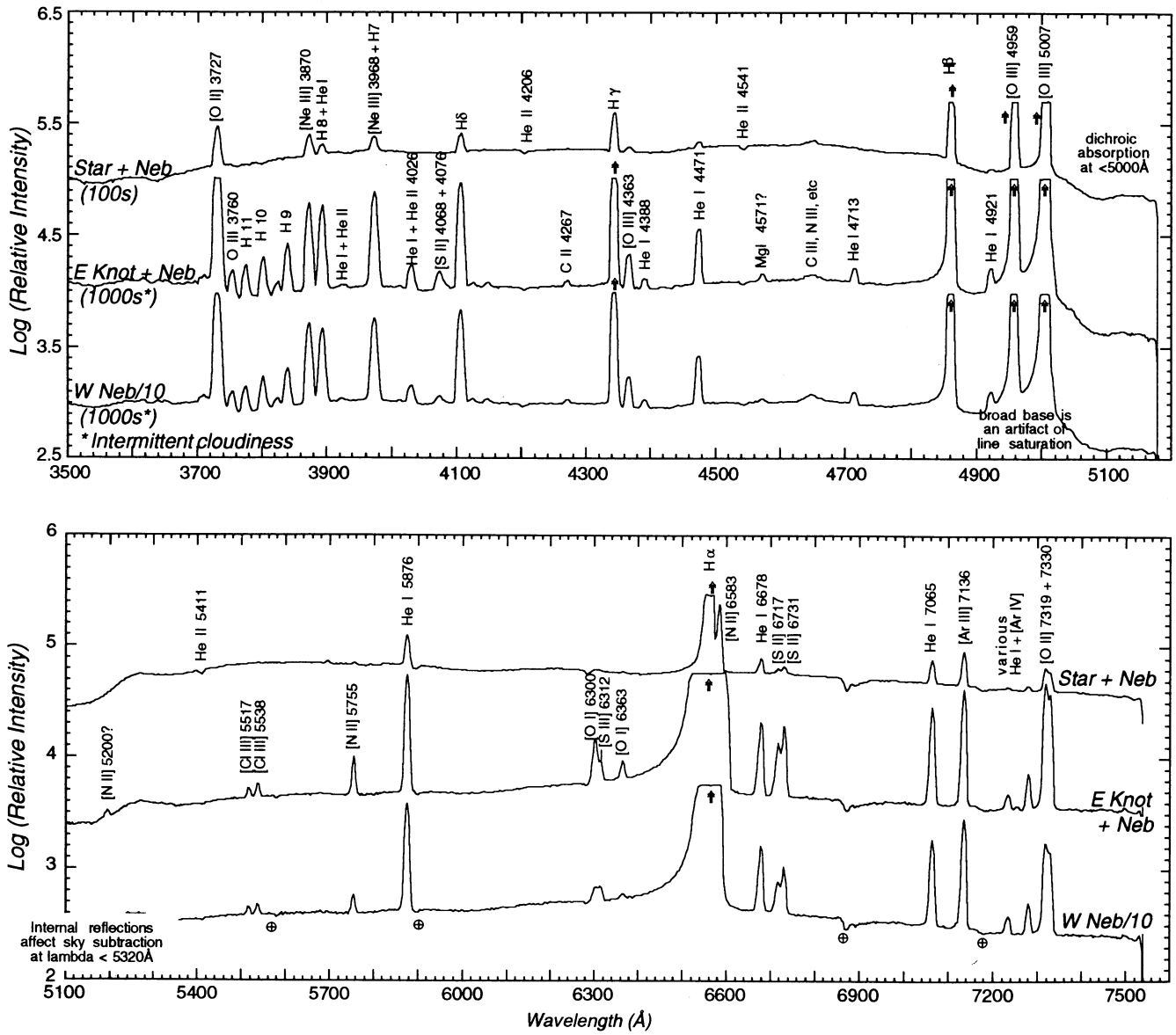

FIG. 11.—Spectra of selected features of IC 2419. See legend to Fig. 3 for other details

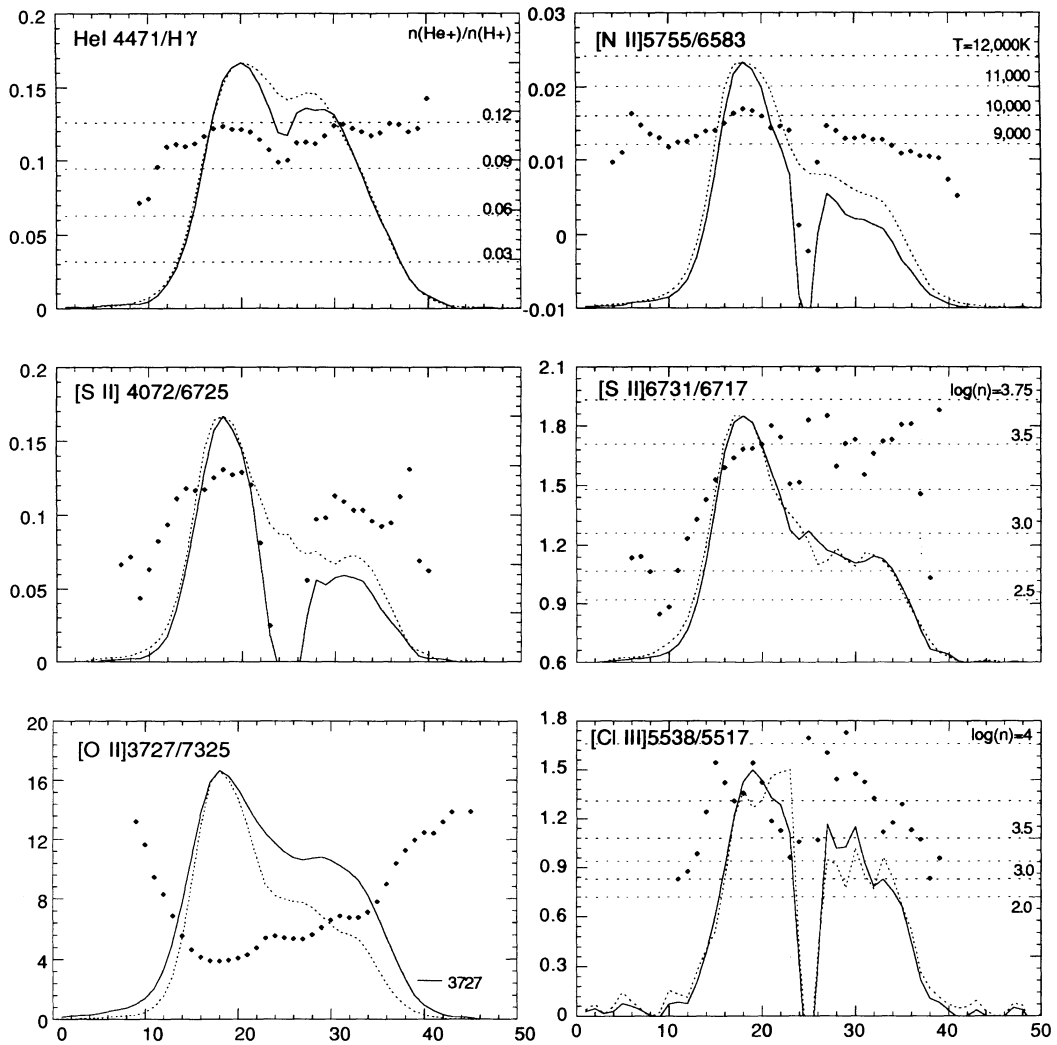

FIG. 12.—Line ratios and normalized slit profiles of the emission lines for IC 2149. See legend to Fig. 4 and the text for other details.

along the slit as seen in NGC 3242 and NGC 7662. In all, the results are much the same as for the other nebulae discussed in this paper, especially NGC 7662.

5.4. *Discussion*

It is worth mentioning in passing that *if* the east knot is a FLIER, then it is a kindred spirit to the south FLIER of NGC 7662. All of our comments regarding the excitation and heating of the south FLIER in NGC 7662 would also apply to the east knot of IC 2149.

6. CONCLUSIONS

The spectral properties of FLIERs in PNs have been explored in this paper. FLIERs are characterized by their knotlike or filamentary shapes (Balick 1987), their kinematics (BPI), and their very low state of ionization. We have found in this paper that the temperatures, densities, and pressures of FLIERs are much the same as the shells of PNs.

The morphologies, kinematics, and spectral properties of FLIERs have been considered in the light of excitation by shocks (such as those important in some HH objects) and by thermal electrons (as in most H II regions). Neither model fits the broad range of observations—especially the low pressures and pressure gradients—particularly well. Shock models, especially bow-shock models, come closer, since they are naturally consistent with the two primary defining attributes of FLIERs: their small sizes and high outflow velocities. Nonetheless, the very low ionizations of the FLIERs are difficult to reconcile with their low densities in the presence of strong stellar ionizing radiation.

An experimentally supported mechanism for producing highly collimated flows that generate FLIERs has yet to be proposed. Soker (1992) has suggested that a common-envelope binary with a low-mass companion can produce ansae and jets with velocities of 50–300 km s^{-1} at various stages of the evolution of the nucleus. The morphological and kinematic properties of these features are nicely in accord with observations. Unfortunately, Soker's calculations do not bear on the issue of the excitation or optical spectroscopic properties; i.e., the present observations are neither a necessary nor a sufficient test of his hypothesis.

No other mechanisms to produce highly collimated polar flows from the nucleus have been proposed for AGB or post-AGB stars. Rather, these mechanisms are generally invoked to account for distended and dense equatorial toroids. The mechanisms include magnetic ejection (Pascoli 1992),

common-envelope binary star ejection (Soker 1990; Soker & Harpaz 1992; see also Morris 1987), and wind compression of rapidly rotating stars proposed for Be stars (Bjorkman & Cassinelli 1993).

Other ideas for collimating flows do not involve the nucleus. BPI suggest that a prolate collisionless shock can cause wind streamlines of the gas to converge toward the symmetry axis. A quasi-stationary and observable standing shock might form along the symmetry axis. The streaming gas has about the right velocity ($\approx 10^3$ km s^{-1}); however, it is also very hot ($\geq 10^7$ K). Unless the gas can become thermally unstable and quickly cool, the converging streamlines quickly diverge. Numerical hydrodynamic models by Icke, Balick, & Frank (1992, hereafter IBF), do not support the formation of FLIERs as a long-lived hydrodynamical process. However, as discussed at length in § 5 of IBF, conditions may be particularly appropriate to FLIER formation as the fast wind starts up. IBF were unable to incorporate the necessary physics to explore this possibility quantitatively. Soker (1990) and Cuesta et al. (1993) reach a similar conclusion based on roughly similar grounds.

Several future directions of research will be fruitful. Most important will be the cleaner kinematic separation of FLIER spectra from those of the local background. In addition, the inexplicably high relative intensities of auroral lines of [S II] and [O II] in NGC 3242 and NGC 7662 (but not in IC 2149) need clarification. The chemical abundances, especially an N-enrichment, might be found if the FLIERs are really recently ejected stellar material. As kindly noted by the referee of this paper, there could be a link between putative abundance anomalies in the FLIERs and the N-rich knots associated with Abell 30 and Abell 78 (cf. Jacoby & Ford 1983).

With respect to the question of thermal versus collisional models, a very useful and potentially decisive test is to search for evidence of emission-line broadening in the stagnation zone at the head of a shock which precedes a bullet or jet into the upstream material. (This has been done successfully for HH objects already, e.g., Solf et al. 1988.) All of these observations can be done with existing echelle spectrographs of Fabry-Perot interferometers.

Observations at Palomar Observatory were made as part of a continuing collaborative agreement between the California Institute of Technology and Cornell University. It is a pleasure to thank the staff of Palomar Observatory for their hospitality and generous help with the observations. We acknowledge the very important resource, the Strasbourg-ESO Catalogue of Galactic Planetary Nebulae (Acker et al. 1992), and thank its authors for their considerable and productive efforts. B. B. is grateful for partial support by grants from the National Science Foundation (AST 89–13639) and the Netherlands Foundation for the Advancement of Pure Research (92/16592). M. R. was supported by the Graduate Student Research Fund of the University of Washington. J. N. C. and Y. T. were supported in part by the National Astronomy and Ionosphere Center, which is operated by Cornell University under a cooperative management agreement with the National Science Foundation.

REFERENCES

Acker, A., Ochsenbein, F., Stenholm, B., Tylenda, R., Marcout, J., & Schohn, C. 1992, Strasbourg-ESO Catalogue of Galactic Planetary Nebulae (Garching: ESO)
Aller, L. H. 1984, Physics of Thermal Gaseous Nebulae (Ap. Space Sci. Library, Vol. 112; Dordrecht; Reidel)
Balick, B. 1987, AJ, 94, 671
Balick, B., Preston, H. L., & Icke, V. 1987, AJ 94, 1641 (BPI)
Barker, T. 1985, ApJ, 294, 193
———. 1986, ApJ, 308, 316
Bjorkman, J. E., & Cassinelli, J. P. 1993, ApJ, 409, 429
Blondin, J. M., Königl, A., & Fryxell, B. A. 1989, ApJ, 337, L37
Chu, Y.-H., Manchado, A., Jacoby, G. H., & Kwitter, K. B. 1991, ApJ, 376, 150
Cuesta, L., Phillips, J. P., & Mampaso, A. 1993, preprint
Frank, A., Balick, B., & Riley, J. 1990, AJ, 100, 1903
Gussie, G. T., & Taylor, A. R. 1989, PASP, 347, 901
Hartigan, P. 1989, ApJ, 339, 987
Hartigan, P., Raymond, J., & Hartmann, L. 1987, ApJ, 316, 323 (HRH)
Icke, V., Balick, B., & Frank, A. 1992, A&A, 253, 224 (IBF)
Jacoby, G. H., & Ford, H. C. 1983, ApJ, 266, 298
López, J. A., Roth, M., & Tapia, M. 1993, A&A, submitted
Morris, M. 1987, PASP, 99, 1115
Morris, M., & Reipurth, B. 1990, PASP, 102, 46
Noriega-Crespo, A., Böhm, K. H., & Raga, A. C. 1989, AJ, 98, 1388
———. 1992, preprint
Pascoli, G. 1992, PASP, 104, 350
Peimbert, M., Sarmiento, A., & Fierro, J. 1991, PASP, 103, 815 (RMM)
Richer, M. G., McCall, M. L., & Martin, P. G. 1991, ApJ, 377, 210
Soker, N. 1990, AJ, 99, 1869
———. 1992, in Proc. Second ESO/CTIO Workshop (La Serena), Mass Loss on the AGB and Beyond, ed. H. E. Schwarz (Garching: ESO), in press
Soker, N., & Harpaz, A. 1992, PASP, 194, 923
Soker, N., Zucker, D. B., & Balick, B. 1992, AJ, submitted
Solf, J., Böhm, K. H., & Raga, A. 1988, ApJ, 334, 229
Wilson, O. C. 1950, ApJ, 111, 279

Note added in proof.—M. Bryce and B. Balick (private communication) have obtained deep long-slit, high-dispersion (3 km s^{-1}) spectra of the Hα and [N II] lines of the FLIERs of NGC 3242 and IC 2149. A small Hα line at the FLIER location and velocity could have been identified in NGC 3242 if it were one-third as bright as the [N II] line. No such feature is seen. In addition, they report that the low-ionization knots of IC 2149, identified as possible FLIERs in the present paper, differ in velocity by only 15 km s^{-1} and do not meet the general criteria to be classified as FLIERs. Bryce and Balick used the Manchester echelle on the 2.5 m Isaac Newton Telescope operated by the Royal Greenwich Observatory in 1992 November.